

A coupled DFE-Newtonian Cellular Automata scheme for simulation of cave initiation, propagation and induced seismicity

Beck, D. A.

Beck Engineering, Sydney, New South Wales, Australia

Sharrock, G.

The University of New South Wales, Sydney, Australia

Capes, G.

Newcrest Mining Limited, Orange, NSW, Australia

Copyright 2011 ARMA, American Rock Mechanics Association

This paper was prepared for presentation at the 45th US Rock Mechanics / Geomechanics Symposium held in San Francisco, CA, June 26–29, 2011.

This paper was selected for presentation at the symposium by an ARMA Technical Program Committee based on a technical and critical review of the paper by a minimum of two technical reviewers. The material, as presented, does not necessarily reflect any position of ARMA, its officers, or members. Electronic reproduction, distribution, or storage of any part of this paper for commercial purposes without the written consent of ARMA is prohibited. Permission to reproduce in print is restricted to an abstract of not more than 300 words; illustrations may not be copied. The abstract must contain conspicuous acknowledgement of where and by whom the paper was presented.

ABSTRACT: Coupled, granular flow-deformation simulations have been undertaken at a number of caving operations to simulate cave initiation, propagation and gravity flow. The tool combines a Newtonian Cellular Automata (NCA) representation of the cave muckpile with an explicit Discontinuum Finite Element (DFE) model of the rock mass. The simulations are three dimensional, mine scale and incorporate high resolution input data such as large numbers of explicit structures in the rock mass and very large numbers of small particles in the cave muckpile. The coupled simulations incorporate:

- Velocity based instability criteria for cave back instability, assessed by the DFE model allowing direct, explicit forecasting of cave propagation geometry and rates.
- Evolution of swell within the cave, computed by the NCA numerical method.
- A physics based equilibrium state between the cave material and the uncaved rock mass computed by the DFE model.
- Changes in load distribution within the cave and across the cave floor arising from the differential flow rates within the cave, consequent to the draw schedule.
- Calibrated, energy based assessment of seismogenic potential.
- Assessment of support performance via assessment of support demand versus capacity.

In this paper, example analysis results are compared to field measurements and interpreted in terms of the relation between modelled and measured draw, muckpile movements, cave growth and subsidence. The modelled stress, strain and energy changes in the rock mass are then used to describe aspects of cave initiation and propagation in terms of rock mass stability and seismicity.

1. INTRODUCTION

Problems with fragmentation, dilution, ore cut-off by waste and propagation, leading to reduced recovery are common in modern caves. Some examples common mechanisms of ore loss are shown in Figures 1, 2 and 3.

In the fictitious example shown in Figure 1, a slope failure induced by the effect of the cave on the pit slope results in mobilization of a volume of material on a scale not much smaller than the cave itself. The majority of the failure may be slow flowing, but compared to a similar cave with no overlying pit, there is a massive amount of additional waste that may dilute the cave and a high risk that some of the waste will cut off, or displace flows of ore. If the failure contains a large

volume of fines, the problem will be worsened and especially difficult to recover from. Such failures are sometimes economically catastrophic.

The example shown in Figure 2 shows primary fragmentation for a conceptual cave, simulated using a DFE model. The model is a strain softening dilatant, Hoek Brown DFE model, calibrated with high fidelity to forecast rock mass damage very well. The fragmentation estimate is based on the simulated plastic work and Bonds law. The model results for a section at the edge of the cave shows how structures concentrate and partition strain, leading to compartments of favorable and poor fragmentation. The well fragmented volumes flow well, but the poorly fragmented areas, while still caved, may not and when breakthrough into the overlying cave

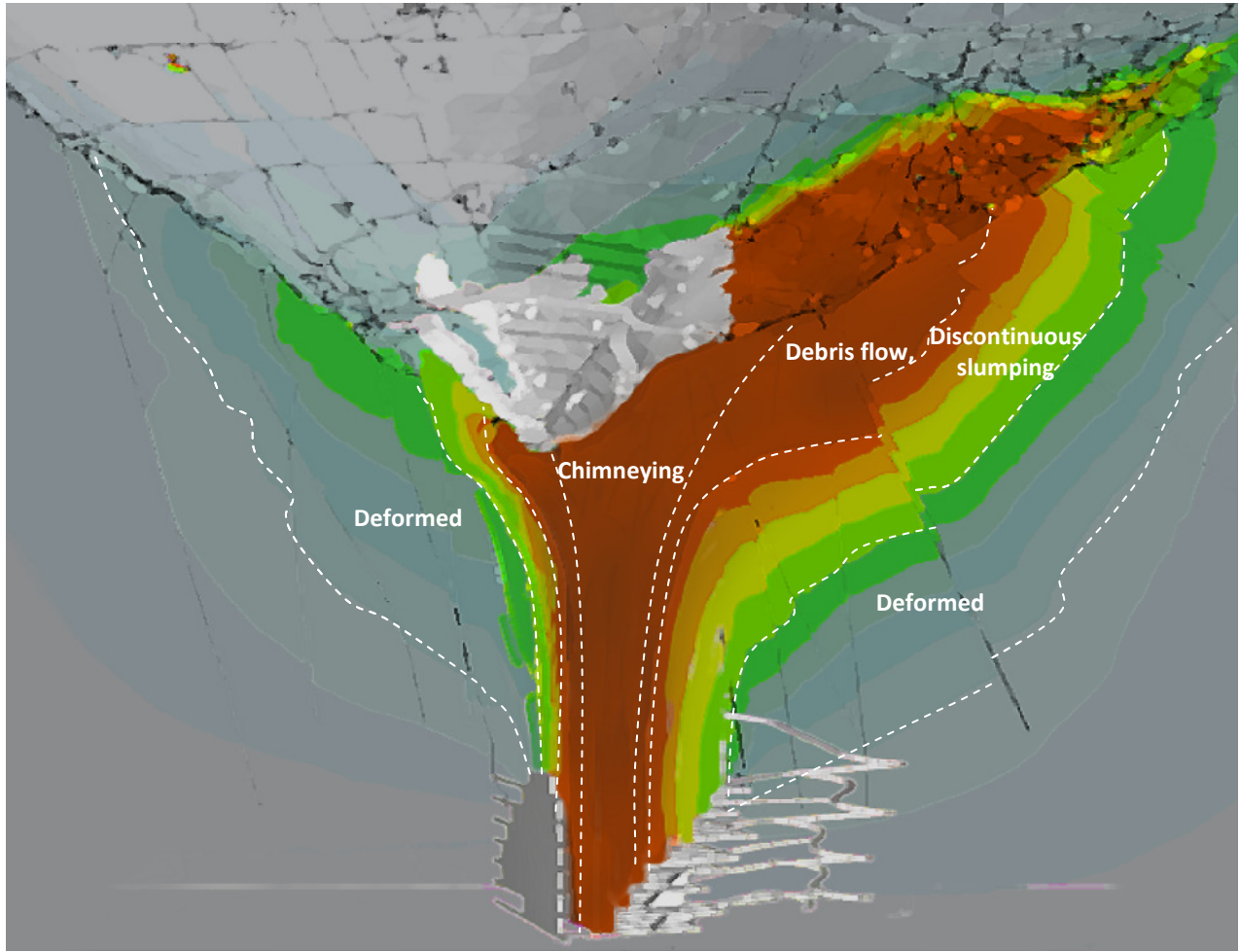


Figure 1 Artists rendition of material movements into a fictional inclined cave, following slope failure. In this case the failure is of a similar scale to the cave.

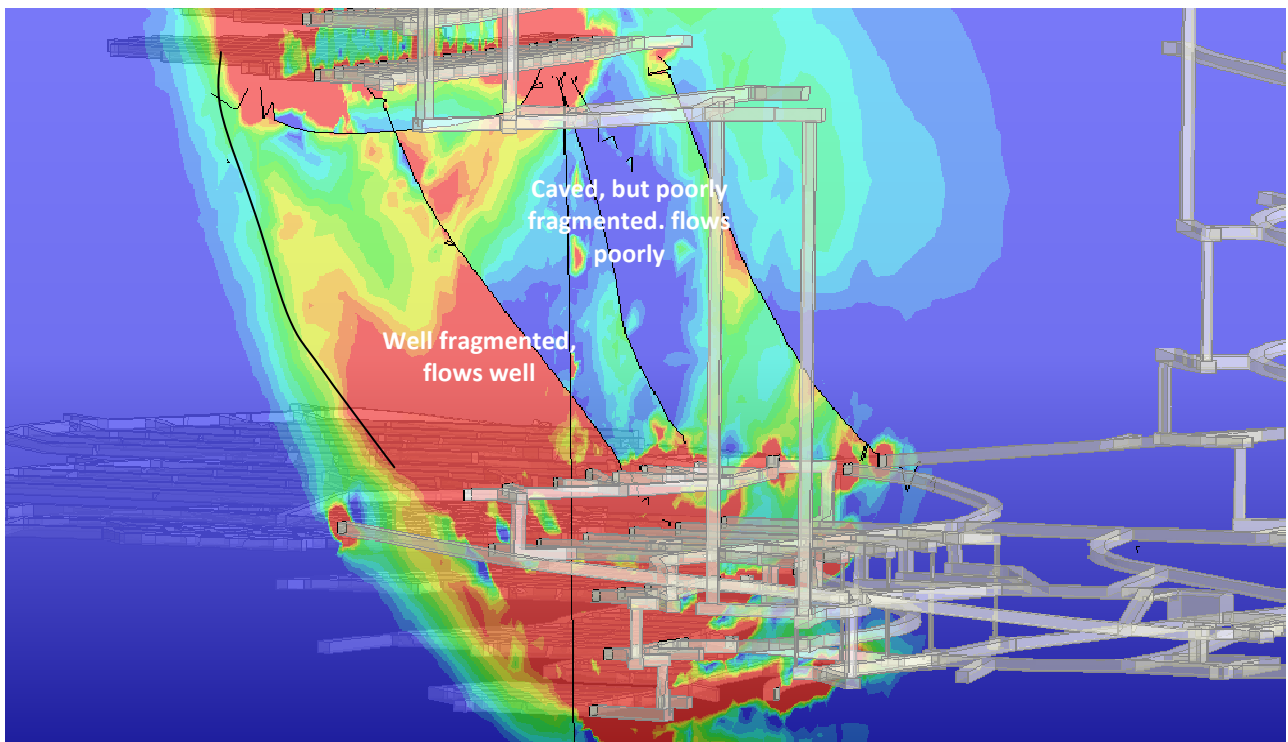


Figure 2 Model forecast fragmentation, on a section near the edge of a discarded block cave concept. A large zone of poorly fragmented material develops due to the influence of structures, the overlying cave and the undercutting direction.

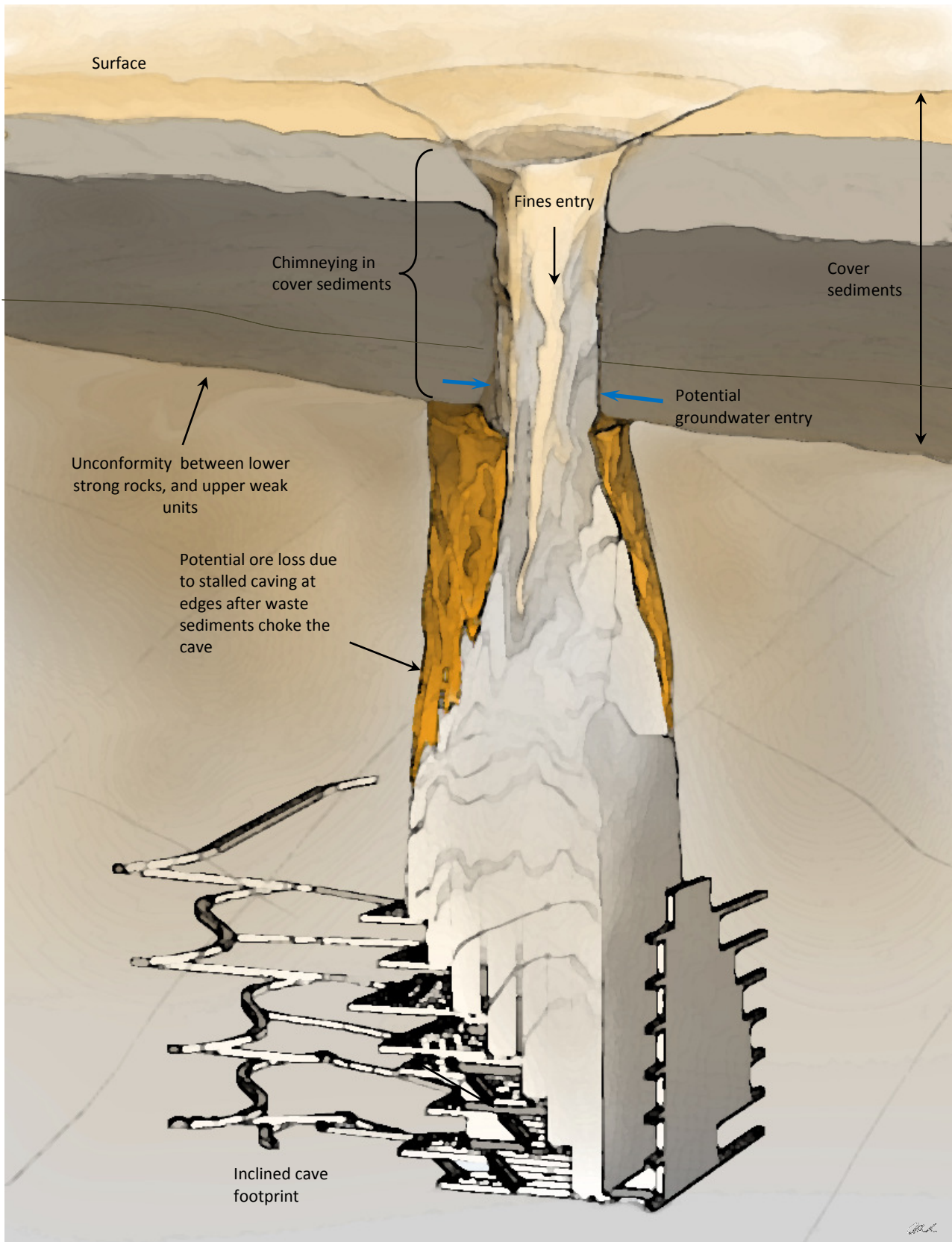


Figure 3 Artists rendition of a mechanisms for choking of the cave by fines, leading to resource loss via non-caving of parts of the column.

occurs, the inflow of that material can choke further propagation of cave. The ore losses can be significant.

The nature of the distribution of the well and poorly fragmented zones also affects how cave loads are distributed. If the poorly fragmented zones act as a catchment for cave loads, the slow moving area may 'point load' and crush the underlying part of the footprint. In practice, this kind of result, partitioned flow of better fragmented zones and structurally induced variability in loads across the footprint, is common, especially where new caves underlie older ones.

In the final example scenario, shown in Figure 3, a fictional cave has broken into a layer of faster flowing waste material. The waste material from higher in the column will flow and rill under the cave shoulders, preventing slumping of these upper corners of the cave, choking further propagation of the ore. The waste will rill along the cave shoulder and to the drawpoints below and the uncaved 'corners' of the cave will not be recovered. It is possible the rock in these areas can disassemble and even technically subside and cave, but the stress path is not favorable for good fragmentation, subsequent flows and recovery of this material. This problem is especially common and is similar to a scenario where a new deeper cave underlies an older cave. In place of the weaker fast flowing surface material, the pre-caved overlying material flows and chokes the cave, limiting recovery of the ore column.

All of these scenarios are artistic renderings of realistic scenarios of ore loss. In each case the effect on cave performance can be catastrophic, so sufficient tools and procedures for assessing the potential for these types of problem are essential for managing planning and production.

2. SELECTION OF MODELLING APPROACH

The examples and the whole family of cave initiation, propagation, dilution and ore cut off by waste problems are driven by an adverse and complex interaction between the discontinuous rock mass outside the cave and the flowing muck pile inside it. Simulating the coupled response of these separate domains is essential if the next generation of super caves are to be properly assessed.

To capture the physics of these mechanisms efficiently, currently requires a hybrid approach, with intermediate outputs of the flow and deformation parts used to constrain successive iterations of the other. A numerical scheme involving simultaneous, parallel solution of the flow and deformation parts would be even more desirable, but computational limits make this less practical in the short term.

Selection of flow and deformation tools for hybrid coupled analysis is described in Beck and Putzar (2011):

- A need for realistic simulation of discontinuous displacements, implying a need for a modeling tool that can represent a large number of explicit discontinuities, the complete 3d geometry and extraction sequence with high fidelity and that incorporates a sufficient constitutive model (arguably only a strain softening, dilatant model, or better). In other words, the extent and magnitude of rock mass damage and deformation must closely match field behavior.
- The flow tool must simulate the flow within the cave rapidly and realistically. This implies that it must also represent the mechanics of movement and swell or bulking sufficiently that flow within the cave can be calibrated to approximate observations on a cave scale.
- The outputs of both parts must be compatible; deformation analysis can only be driven by forces, displacements and material state changes, so the flow code results must be in this form.
- The analysis must be efficient and able to be computed in a short period to allow multiple runs for back analysis and calibration as well as integration with mine planning and operations (Beck and Lilley 2011). For the case study summarised below, the problem required over 10 million degrees of freedom for the rock mass part and over 60 million particles and weekly excavation steps.

This combination of fundamental considerations and size led to the development of a coupling scheme for the Explicit Discontinuum Finite Element (DFE) program (Abaqus Explicit, Simulia 2010) for the deformation part and a Newtonian Cellular Automata (NCA) code (CaveSIM, Sharrock 2010) for the flow part. Later, the Scheme was adapted to include an interface between the DFE code and other Lattice Grain Cellular Automata tools. A number of other valid potential combinations exist, but only the DFE-NCA coupling and related examples are described here.

3. DFE/NCA COUPLING MECHANISM

As the NCA code is currently unable to output forces or stresses, the coupling mechanism between the flow code and DFE part relies on the DFE part to replicate the stiffness changes in the cave that result from NCA computed muck pile movements and shape.

The current coupling procedure implemented in this way is as follows, after Beck and Putzar (2011):

- 1) The DFE model generates an unstable zone, as a consequence of its solution for particular excavation step. For example, at the end of a prior step, complete at time T, the DFE model provides an estimate of the unstable zone that is likely to make the transition from loosened rock mass to cave

material over the following coupling period of time length (t_c), set as small as computationally possible.

- 2) The criterion for instability in the DFE model was based on velocity: above a critical velocity (V_{crit}) material can be considered unstable (see for example Reusch et al 2010). The particular value for V_{crit} was established in the calibration stage by comparing node velocity in the DFE model to actual increments of caving.
- 3) At time T , the DFE model rests while NCA simulates the 'falling' of the unstable zone and the drawing of the material scheduled for the whole of time t_c .
- 4) When the muckpile in NCA comes to rest, or is sufficiently still after drawing the production for the period T to $T + t_c$, the new cave shape predicted by the DFE/critical node velocity part is then allowed to develop in the DFE part, guided by the NCA result as follows:

- a. Between T and $T + t_c/4$
 - i. New open tunnels excavated at this time in the schedule are transitioned from rock mass, to unsupported excavation and where applicable to supported excavation over $t_c/4$.
 - ii. Newly blasted undercut rings for the time period T to $T + t_c$ are ramped down to the stationary cave modulus (a calibrated value).
 - iii. All new or old muckpile or airgap, as originally defined using the instability criterion transitions to a transitional modulus state (a calibrated value).

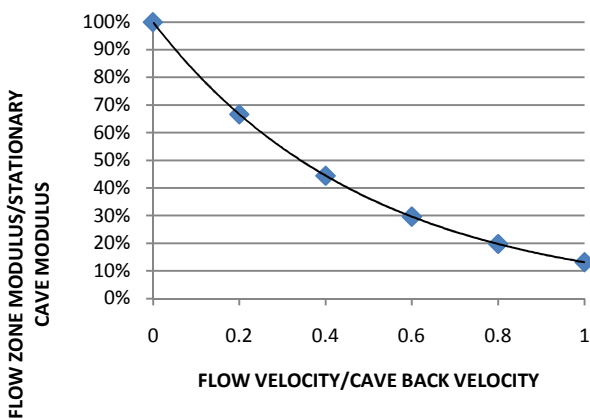


Figure 4. Example assumed relation between flow zone modulus and stationary cave modulus, based on flow velocity. This curve is calibrated as part of the calibration procedure.

- 5) The value of the transitional modulus of cave elements achieved at $T + t_c/4$ varies node by node based on the velocity of each corresponding node in the NCA model. The relationship that defines the modulus of mobile material compared to stationary

cave material, as a function of flow velocity and cave back velocity is shown in Figure 1. This relation was developed using empirical and anecdotal data during the calibration.

- 6) The gradual change from current to new modulus over the time period $t_c/4$ aids numerical stability of the model.
 - a. Between $T + t_c/4$ and $T + t_c/2$:
 - i. The modulus of elements indicated to be airgap by NCA continues to be ramped down to the air modulus (near zero).
 - ii. the modulus of muckpile material - new and old is held at the transitional state, i.e. based on the velocity from NCA and the modulus from the relationship in Figure 4.
 - iii. New excavations for that period are mined in the usual way (ramped down to air then ramped up to the support modulus).
 - iv. New undercut for that period is ramped down to stationary cave material as before.
 - b. Between $T + t_c/2$ and $T + 3t_c/4$:
 - i. The modulus of mobile parts of the muckpile are ramped back up to the modulus of stationary cave.
 - ii. Airgaps are left at the air modulus (near zero).
 - iii. New excavations for that period are mined in the usual way (ramped down to air, ramped up to the support modulus).
 - iv. New undercut for that period is mined as before.
 - c. Between $T + 3t_c/4$ and $T + t_c$:
 - i. Cave and airgap modulus are held steady.
 - ii. New excavations for that period are mined in the usual way (ramped down to air, ramped up to the support modulus).
 - iii. New undercut for that period is mined as before.
 - iv. The model reaches quasi-static equilibrium for the most part - some small areas above airgaps may still be moving at the end of the period in theory but this did not occur in this model.
 - d. A new unstable zone is generated, using the instability criterion, and this shape is transferred to the NCA part for the next iteration.

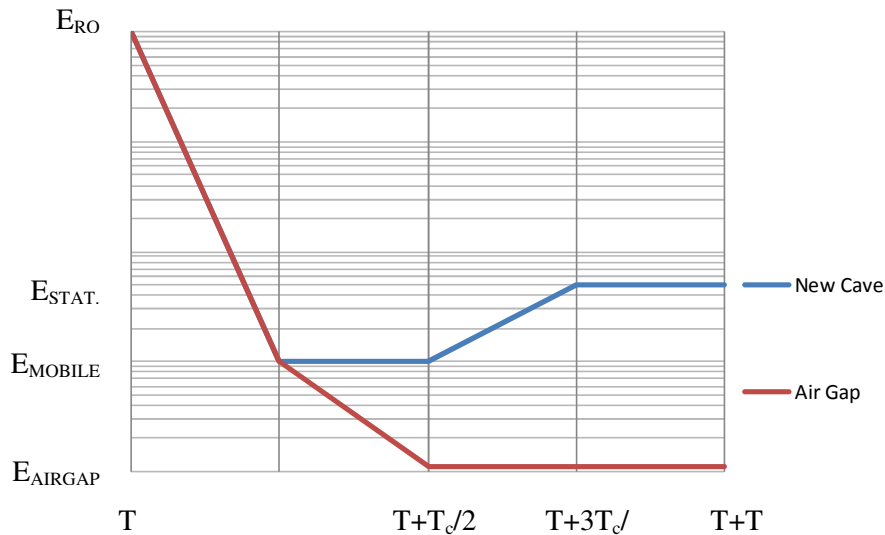


Figure 5. Modulus transitions in the DFE model in a coupling step for new cave - muck pile or air gap. E_{MOBILE} is based on the relationship shown in Figure 1, dependent on the modeled particle velocity. E_{RO} is the modulus of the rock before entering the cave

7) The process repeats.

The procedure of cave modulus change to represent draw effects is represented on a schematic timeline for a single DFE step, for rock entering the cave in the coupling cycle in Figure 5.

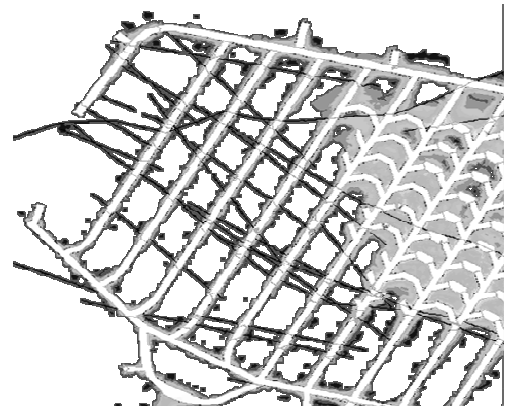
4. EXAMPLE APPLICATION

The coupling procedure was applied to the analysis of interaction between a new Block Cave (BC) and a Sub Level Cave (SLC) at Newcrest Ridgeway Mine for the purpose of assessing the potential for risks like those outlined above. The model details are summarized in Table 1 and discussed in Beck and Putzar 2011. An example of the density of explicit structures included in the model is shown in Figure 6, also after Beck and Putzar, 2011.

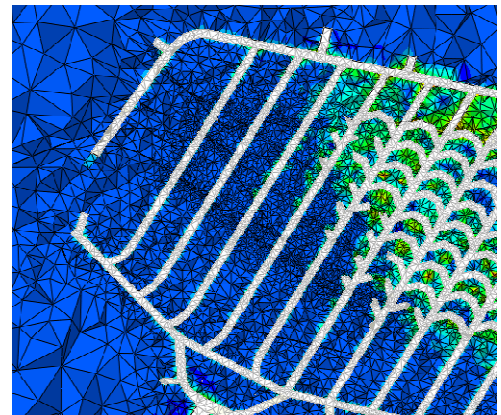
To calibrate the model, the coupling parameters and rock mass and discontinuity properties were adjusted over successive iterations to achieve a quantifiable match to field measurements. The intent is to match the measured and modeled variables as directly as possible: Dissipated Plastic Energy to Seismic occurrence, the timing and magnitude of modeled and measured damage, the location of the cave back in 3d and damage models from passive tomography to plastic strain in the rock mass.

During calibration, the resolution, precision and efficacy of the model for the intended purpose is established. This includes establishing a procedure for future use of the model. In the example case, because the simulation results are produced in simple measures such as displacement or tunnel damage, they are conceptually accessible; all members of the team can directly appraise them. This combination of model forecasts presented using field measurable quantities, and results accessibility leads to transparency. If the results are not matching observations, this becomes immediately

apparent. All team members with access to the data have the opportunity to identify model-field incongruities which is important, as no single member of a planning team can observe the entire mine at once, and certainly not through the eyes of the collective experience of the entire team.



(i)



(ii)

Figure 6. Example of (i) typical scale and density of discontinuities (solid lines) built in the mine scale model and higher order FE mesh density.

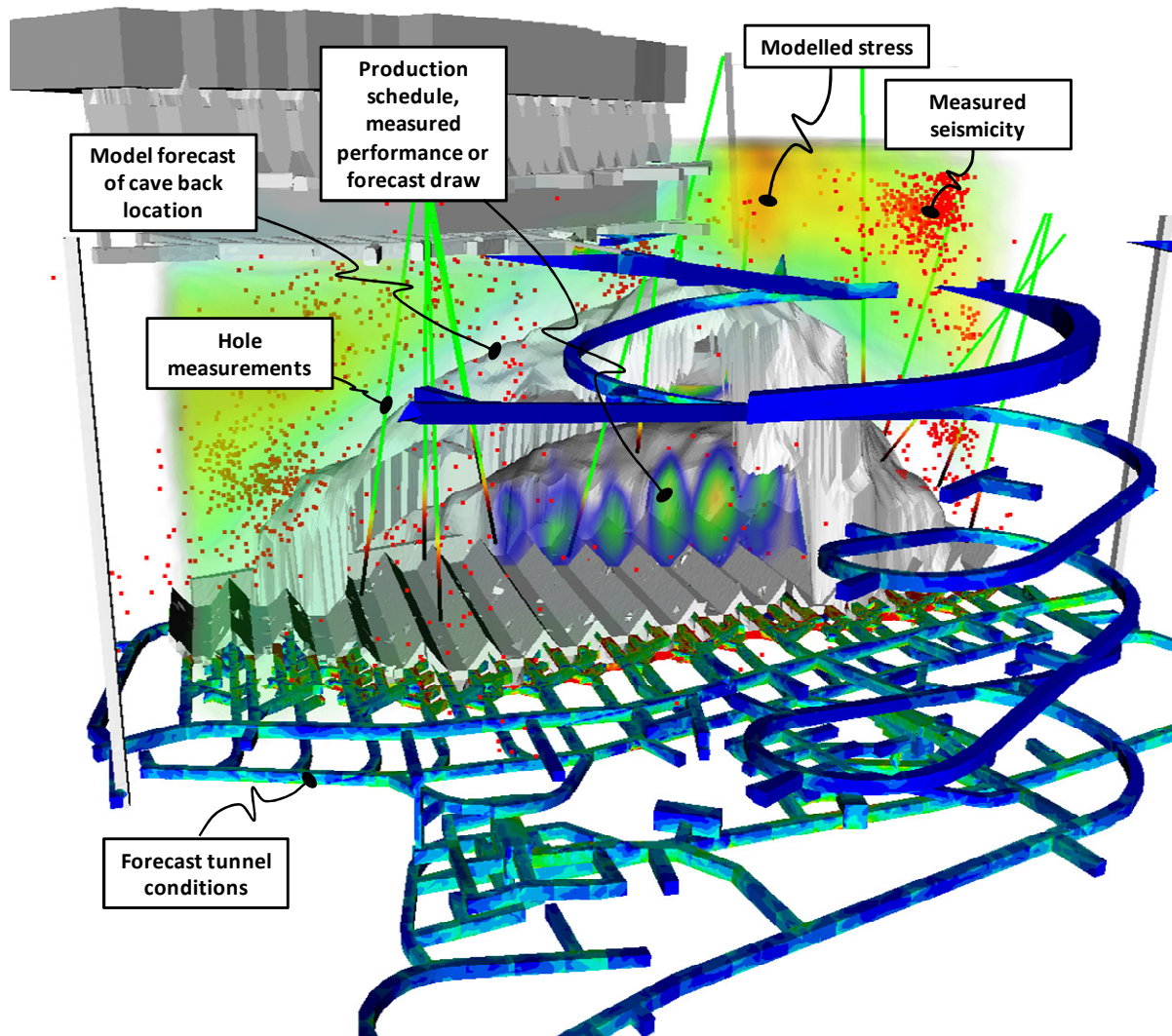


Figure 7. Example of data from multiple sources visualized in a 3d collaborative workspace. The layering of modeled and measured data aids rapid model calibration, validation and improvements, as well as appreciation of developing issues. The collaborative approach is possible because the model precision and resolution has been estimated during the calibration process and the model has been deemed sufficiently reliable.

In the case of a mismatch between the model and field measurements, either a scenario is playing out in real life that was not forecast and action is needed (plan modification or a hazard reduction strategy), or the simulation tool needs adjustment, and the observed incongruity becomes a data point for calibration and re-analysis.

An example image showing how modeled and measured data are compared qualitatively during operations is shown in Figure 7, after Beck and Lilley 2011. This figure shows a combination of measured and modeled data: measured seismicity and rock mass changes viewed in open holes, compared to model forecasts of stress, cave back locations and forecast tunnel conditions, extensometer data and NCA forecasts of cave flows. In this example, anything which the mine measures, and anything which its engineering tools forecasts, and any design or schedule that the planning

team proposes can be viewed in one workspace to validate the model and drive continuous improvements.

Examples of model forecasts, compared to field data are shown in Figures 8, 9 and 10. Figure 8 shows an example match between modeled and measured seismic events. The close match is representative of the model performance during each month of the study period. Figure 8 shows a comparison between forecast and measured cave location. The open holes used to measure the cave location are colored black within 20m of the cave back to indicate where the model error is less than 20m. The model was at least this accurate for every open hole and was able to accurately predict the timing and location of the BC breakthrough into the overlying SLC with an error of less than 1 month. The final comparison of modeled and measured data shows modeled and measured damage to ground support (Figure 10). This kind of plot can be used to plan rehabilitation during

operations, or to estimate the demand on ground support in different parts of the footprint during planning.

Ultimately, the close match between the forecasts and measured data validated the tool for its intended use, to assist the mine in planning draw strategies. Most importantly, the tool was able to match the cave propagation and was deemed sufficiently reliable for assessing risks of the type shown in the examples of Figures 1, 2 and 3.

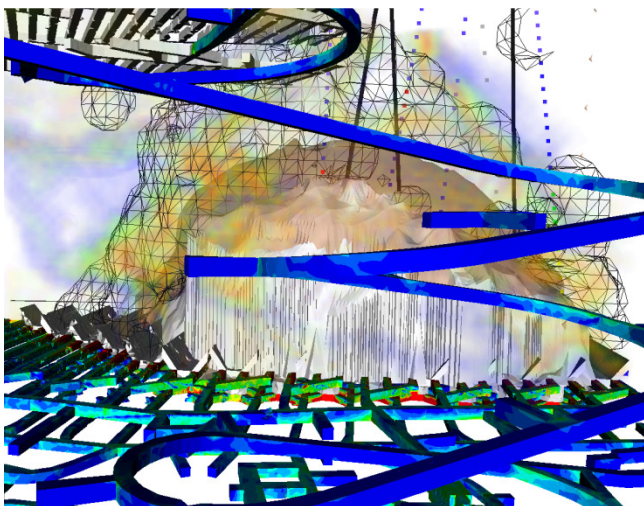
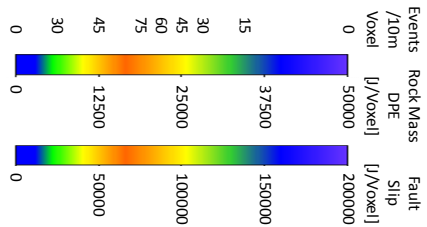


Figure 8. Comparison of modelled (contours) and measured (wireframe) event densities, after Beck and Putzar 2011.

5. CONCLUSIONS

The coupled DFE-NCA simulation procedure enables rapid simulation of cave propagation, flow and induced deformation, driven by the cave draw schedule. The method can be calibrated directly using observations of cave back location, grade and recovery, seismicity, tunnel damage, tomography and or ground movement.

At several mines, including Newcrests Ridgeway Mine, the results of DFE-NCA analysis closely conformed with field measurements suggesting the technique is useful for forecasting, and is especially useful for assessing cave propagation risks.

6. ACKNOWLEDGEMENTS

The authors wish to thank Newcrest Mining Limited for permission to publish the example results from Ridgeway Mine, and especially David Finn for considerable assistance during the modelling project. The authors also wish to thank Gero Putzar for supervising the final coupled simulation and Patrick Bartlett and Richard Butcher for technical advice.

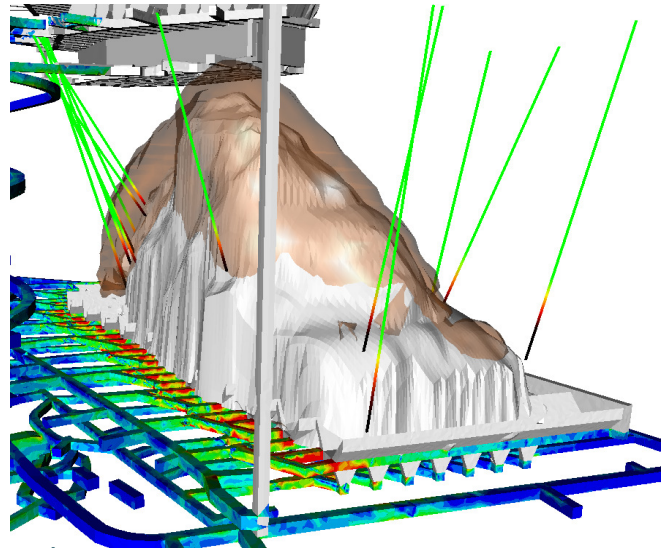
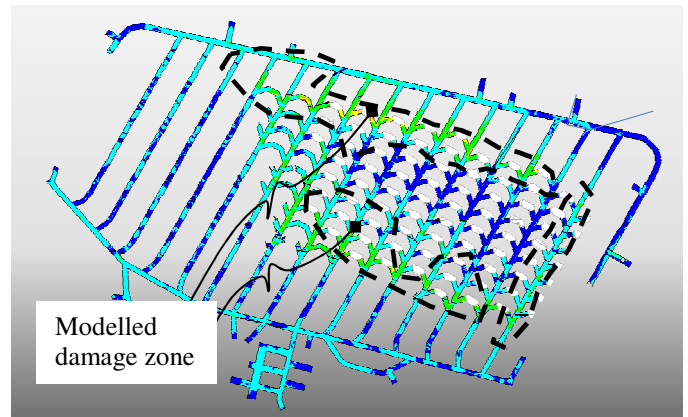


Figure 9. Comparison of forecast cave shape (grey/brown solid) and actual cave shape observed in monitoring holes/ the black tails on the holes indicate the last 20m of the measured hole, indicating a forecast accurate within 10-20m across the entire cave, after Beck and Putzar 2011.



(i)



(ii)

Figure 10. Comparison of (i) modelled and (ii) measured extraction level damage for an example time period. The model correctly forecasts the minor damage seen at the mine, both in extent and magnitude.

REFERENCES

1. R.G. Jeffrey, A.P. Bungler, B. Lecampion, X. Zhang, Z.R. Chen, A. van As, D.P. Allison, W. de Beer, J.W. Dudley, E. Siebrits, M. Thiercelin, and M. Mainguy. 2009. Measuring Hydraulic Fracture Growth in Naturally Fractured Rock. SPE Annual Technical Conference and Exhibition. New Orleans, Louisiana, USA, 4–7 October 2009. Society of Petroleum Engineers
2. Beck, D.A. and Putzar, G. 2011. Coupled Flow-Deformation Simulation for Mine Scale Analysis of Cave initiation and Propagation. In proceedings of the International Society of Rock Mechanics 2011 Conference, Beijing.
3. Reusch, F., Levkovitch, V. & Beck, D. 2010: "Multi-scale, non-linear numerical analysis of mining induced deformation in complex environments" in "Rock Mechanics in Civil and Environmental Engineering" , Jian Zhao (Editor), Vincent Labiouse (Editor), Jean-Paul Dudt (Editor), Jean-Francois Mathier (Editor), CRC Press, 2010, 697-700.
4. Beck, D.A., Reusch, F. & Arndt, S., 2007. Estimating the Probability of Mining-Induced Seismic Events using Mine-Scale, Inelastic Numerical Models. Intl. Symposium Deep and High Stress Mining 2007. The Australian Centre for Geomechanics, Perth, Australia
5. Beck, D. A., Reusch, F. and Arndt, S. 2009. A numerical investigation of scale effects on the behavior of discontinuous rock. ARMA, American Rock Mechanics Association Symposium. ARMA 09-145
6. Beck, D. A. and Lilley, C. 2011. Simulation Aided Engineering: integration of monitoring, modelling and planning. In proceedings of 11th AusIMM Underground Operators Conference 2011. Canberra, Australia. Published by The Australasian Institute of Mining and Metallurgy.

Table 1 Details of the DFE part of the example coupled model

Feature	Summary	
Deformation Model	3D, strain softening, dilatant, Explicit Finite Element. Cohesive elements as interface elements at boundaries between layers. Higher order tetrahedral elements for rock units	
Discontinuities	Contact/ Cohesive Elements	Major contacts between lithologies modeled as combined cohesive/contact elements. Lesser contacts modeled as cohesive elements or ubiquitous structure
Flow Model	Lattice Grain Cellular Automata	
Simulation packages	Abaqus 6.8 Explicit, CaveSIM	
Constitutive model for the rock mass	Yield potential: Plastic strain potential: Softening:	Menetrey and Williams (1995) with $e=0.6$ to approximate the Hoek-Brown (1980,1992) potential Menetrey and Williams (1995) Piecewise as a function of strain for dilation, cohesion, friction. Menetrey and Williams (1995)